Article citation info:
KOSMOL J. An extended model of angular bearing - influence of fitting and pre-deformation. Eksploatacja i Niezawodnosc – Maintenance and Reliability 2019; 21 (3): 493–500, http://dx.doi.org/10.17531/ein.2019.3.16.

Jan KOSMOL

# AN EXTENDED MODEL OF ANGULAR BEARING - INFLUENCE OF FITTING AND PRE-DEFORMATION

# ROZSZERZONY MODEL ŁOŻYSKA TOCZNEGO – WPŁYW PASOWANIA I ODKSZTAŁCENIA WSTĘPNEGO*

*The paper presents a modeling of angular bearing in the context of motion resistance. It was assumed that the motion resistance depends on the contact forces. For that reason, the main goal of modeling was an estimation of the forces and determination of the influence of such parameters, like rotational speed of the bearing ring, pre-displacement of the bearing and fit of the shaft and the inner ring, exerted on those forces. In the literature, when estimating the contact forces, such parameters are taken into account very rarely. The modelling was performed by means of a numerical method, viz. FEM. The modeling results show that the omission of such parameters will lead to big errors in estimation of contact forces, and those errors may be as high as 100%, or even higher. The real motion resistance will be bigger than calculated.*

***Keywords**: angular bearing, motion resistance, FEM.*

*W artykule przedstawiono modelowanie łożyska tocznego skośnego w kontekście oporów ruchu. Ponieważ przyjęto, że opory ruchu są proporcjonalne do sił kontaktowych to głównym celem modelownia stało się oszacowanie ich wielkości oraz określenie wpływu takich parametrów jak prędkość obrotowa pierścienia łożyskowego, wstępne odkształcenie łożyska i pasowania wałka i pierścienia łożyskowego na te siły. W literaturze tematu parametry te są rzadko albo w ogóle nieuwzględniane przy szacowaniu sił kontaktowych. Modelowanie przeprowadzono metodą numeryczną MES. Wyniki modelowania pokazują, że pomijanie ww. parametrów prowadzi do błędnego oszacowania sił kontaktowych, tj. do ich zaniżania, a błędy mogą sięgać 100% i więcej. W rezultacie rzeczywiste opory ruchu będą większe od oszacowanych na drodze numerycznej.*

***Słowa kluczowe**: ożysko toczne, opory ruchu, MES.*

## 1. Introduction

The development of HSC (High Speed Cutting) technology results in a significant increase in kinematic parameters in the cutting process, viz. cutting and feed speed. In comparison to the cutting parameters hitherto used, the speed increase ranges from a few to a dozen or several dozen times, which has specific consequences, also for the machine tool construction. The increase in the spindle speed results in a significant increase in dynamic forces, among others, in bearing assemblies. Therefore, the quantity of heat in these assemblies will increase, which often forces the constructors of machine tools either to add a new or rebuild the existing cooling system. The addition of a cooling system or its redesigning will entail, first of all, the knowledge of the quantity of heat generated therein.

In the available literature on the subject, a vast majority of reports concern the issue of fatigue life of rolling bearings. It is understandable, since rolling bearings often belong to the weakest elements of the mechanical system. In [5], the authors considered the issue of bearing radial play, but in the context of its durability. By using simulation methods, they tried to determine its best value available. In [16], the authors considered not only the impact of design and construction factors, but also technological and operational factors such as the correctness of assembly, monitoring the balancing of the machine or the effect of lubrication correctness upon the fatigue life of the bearing. In [15], the authors investigated the influence of pre-clamping of angular bearings on their fatigue life. The authors also pointed out that as of today there is no universally available method to select this pre-load.

Instead, this article focuses on the impact of motion resistance in rolling bearings on the operational quality of cutting machine tools. This operational quality, understood as the workmanship accuracy of a workpiece on the machine tool is, among others, closely related to thermal deformations caused by the heat generated in bearings.

It is generally assumed that the quantity of heat generated in the bearing itself is equal to the power of losses resulting from the resistance of bearing motion. The estimation of such a resistance in the bearing is not fully resolved. Commonly, the aforesaid resistance is estimated with Palmgren model [14], according to the formula:

$$\mathrm{M}_1 = z\left(\frac{F_s}{C_s}\right)^y F_\beta d_m$$
$$F_\beta = 0.9F_a\, ctg\alpha - 0.1F_r \qquad (1)$$

where:

$M_1$ – motion resistance torque in a rolling bearing,
$F_s$ – replacement load on the bearing,
$C_s$ – static bearing capacity of the bearing,
$z$ – coefficient dependent on the type of bearing and lubrication (for a deep-groove angular-contact ball bearing) $z$=0.001 [6]),
$d_m$ – average diameter of the bearing,
$y$ – coefficient dependent on the type of bearing and lubrication (for a deep-groove angular-contact ball bearing) $y$=0.33 [6]),
$F_a$ – axial component of external bearing load,
$F_r$ – radial component of external bearing load,

(*) Tekst artykułu w polskiej wersji językowej dostępny w elektronicznym wydaniu kwartalnika na stronie ***www.ein.org.pl***

α – angle of bearing operation.

As it appears from equation (1), it does not explicitly include, among others, the effects of the rotational speed of the bearing (in the Palmgren rule, $M_1$ means only the moment of friction from the external load without centrifugal forces, gyroscopic torque, etc.).

In an angular bearing, at least the following rotary movements will occur (Figure 1):

- the orbital velocity of the balls $\omega_m$, i.e. the rotational movement around the bearing axis on the bearing raceways,
- rotational speed of the inner bearing ring ω,
- rotational speed of balls around their own axis $\omega_B$,
- rotational speed of balls around their own axis $\omega_s$,
- rotational speed of balls $\omega_{roll}$, as a result of gyroscopic torque $M_g$.

Rotational movements in an angular bearing will cause dynamic forces, such as centrifugal forces $F_c$ from orbiting balls, centrifugal forces $F_{cp}$ from the rotating ring, gyroscopic torque $M_g$, resulting from the orbital motion of the balls in the plane deviating from the plane of the bearing by an angle β (this angle changes with the change of the rotational speed of the bearing), the spinning torque of the $M_s$ as a result of the rotational movement of the balls around their own axes.

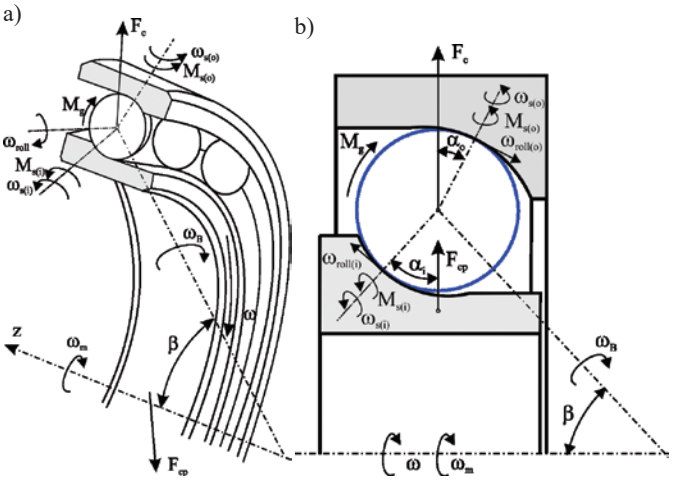


*Fig. 1. Angular bearing rotational movements: ω – rotational speed of inner ring, $\omega_m$ – orbital speed of balls, $\omega_s$ – rotational speed of balls around own axis, $\omega_B$ – rotational speed of balls around own axis, $\omega_{roll}$ – rotational speed of balls due to gyroscopic phenomenon, $\alpha_i$, $\alpha_o$ – contact angels, β – ball pitch angle, $M_g$ – gyroscopic torque, $F_c$ – centrifugal load due to orbital movements of balls, $F_{cp}$ – centrifugal load due to rotational movements of inner ring, $M_s$ – friction torque due to spinning effect*

Figure 2 features a hypothetical state of load in an angular rolling bearing. The total motion resistances of the $M_{op}$ consist of the frictional resistance of balls with $M_{1(T)}$, raceways, sliding friction resistance due to the rotation of balls around their own axis $M_s$, resistance to movement due to the presence of grease $M_v$. This article focuses only on the movement resistance caused by the friction of the balls against the raceways $M_{1(T)}$.

An effect generated by the occurrence of these dynamic forces is, among others, a change in the bearing motion resistance of the $M_{op}$. These effects are not included in equation (1).

A significant increase in speed in HSC machine tools no longer allows neglecting dynamic effects while estimating motion resistance (for the previously used technologies, dynamic effects were omitted, because their impact on motion resistance was small). Hence the necessity to develop a new model for determining the motion resistance in which dynamic effects that affect the bearing motion resistance would be clearly exposed.

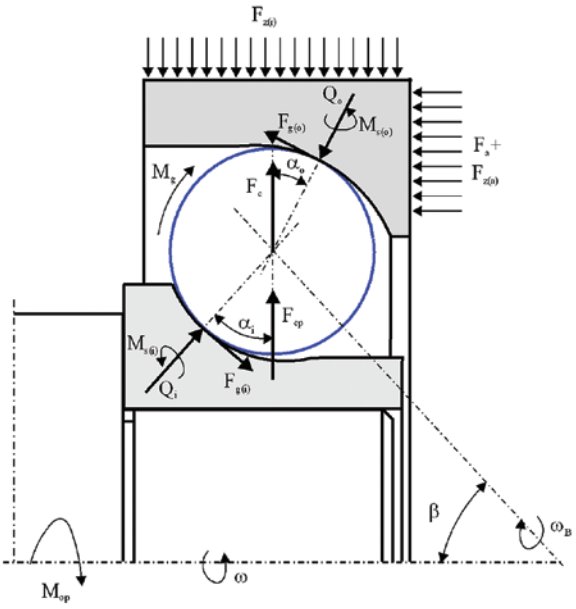

*Fig. 2. Hypothetical state of loads of an angular bearing; $F_{z(r)}$, $_{z(a)}$ – external, radial and axial loads of a bearing, $F_c$, $F_{g(o)}$, $F_{g(i)}$ – dynamical loads – centrifugal and gyroscopic, $M_g$ – gyroscopic torque, $F_a$ – pre-load of a bearing, $M_s$ – spinning torque, $M_{op}$ – friction torque due to load, $Q_i$, $Q_o$ – contact loads*

The author assumed in his monograph [9] that the motion resistance resulting from the effect of friction in a rolling bearing is a function of the dynamic contact forces $Q_i$ and $Q_o$, occurring between the balls (rollers) and bearing raceways as well as of the friction coefficients. To calculate the motion resistance due to rolling friction forces $M_{1(T)}$, the author used the formula presented in [12], viz.:

$$M_{1(T)} = \left(\frac{d_m}{D} + 0{,}5\right) \sum_{j=0}^{j=Z-1} \left(Q_{ij} f_{kij} + Q_{oj} f_{koj}\right) \tag{2}$$

where:

$Q_i$, $Q_o$ – contact forces between the ball and the inner (i) and outer (o) raceway,
$f_{ki}$, $f_{ko}$ – coefficients of rolling friction between the ball and the inner (i) and outer (o) race,
$D$ – ball diameter,
$Z$ – number of bearing balls,
$M_{1(T)}$ – moment of friction caused by the balls rolling on the raceways.

In the literature [1-2], [4], [6], [8-9], [11], [13] can be found many analytical models, allowing one to determine dynamic forces $Q_i$ and $Q_o$ as a function of rotational speed, initial angular bearing pre-load $F_a$ or external load $F_z$. A common feature of these models is the fact that they only take into account the dynamic effects resulting from the orbital motion of the balls around the bearing axis (centrifugal forces $F_c$) and the rotation of the balls around their axes (gyroscopic effect) in the form of the so-called gyroscopic torque of $M_g$.

The author [10] proposed an extended contact model of an angular bearing in which he took into account the dynamic effect resulting from the rotary motion of the gyrating inner ring in the form of centrifugal force $F_{cp}$.

## 2. Extended contact model of the bearing

As already mentioned, most contact bearing models found in the literature do not take into consideration the dynamic effects resulting from the rotational movement of the inner ring. Exceptions include items [3], [7], [18, 19].

The authors [3], [7], [18, 19], while analyzing the state of bearing load resulting from the centrifugal forces of spinning balls, also took into account the deformation of the inner ring due to its rotational speed. What seems to be debatable or unacceptable is the fact that into the equations describing the displacements and deformations in the contact areas those authors inserted displacements of the inner ring, calculated according to the formula corresponding to the freely expanding gyrating ring. It seems that the assumption of the free expansion of the outer surface of the inner ring is erroneous, as this ring is in contact with many balls which takes away its degrees of freedom. In a further part of Chapter 2 of the article presented is the difference in displacement of the ring between the ring subject to free expansion and the ring constituting the bearing element.

Figure 3 presents the phenomenological models, respectively, of a bearing in which the expansion of the inner ring has been omitted (Fig. 3a) and of a bearing in which this expansion has been taken into account (Fig. 3b).

The main difference lies in the model of the susceptible inner ring, $K_r$, which moves radially by a size $\delta_P$. For this reason, in the equation of the equilibrium of forces acting on the inner ring in the vertical direction (depending on (3), there will occur as well an additional force $F_r$, which is proportional to the displacement $\delta_P$. Figure 4 shows the bearing load condition taking into account the centrifugal force from the gyrating $F_c$ balls and the rotating inner ring $F_{cp}$.

For the phenomenological model as in Fig. 4, provided are some equations of forces acting on the ball and the inner ring, namely:

$$\begin{aligned} Q_i \sin\alpha_i &= Q_o \sin\alpha_o \\ F_c &= Q_i \cos\alpha_i - Q_o \cos\alpha_o \\ F_a &= Q_i \sin\alpha_i \\ F_a &= Q_o \sin\alpha_o \\ F_{cp} - F_r - Q_i \cos\alpha_i &= 0 \\ F_r &= K_r \delta_P \end{aligned} \tag{3}$$

and so-called a geometric condition that binds together contact deformations $\delta_i$ and $\delta_o$ and radial displacements of the ring $\delta_P$ (Fig. 4b):

$$(r_i+\delta_i-0{,}5D)\cos\alpha_i+(r_o+\delta_o-0{,}5D)\cos\alpha_o=A\cos\alpha+\delta_P \tag{4}$$

where:

$r_i$, $r_o$ – radii of inner and outer race curves,

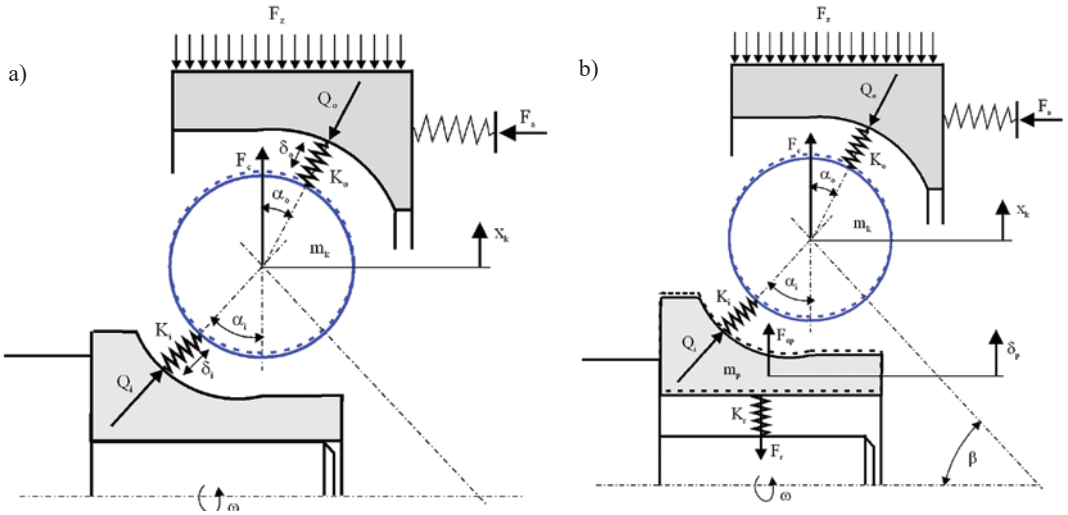


*Fig. 3. Contact models of a bearing: a) without inner ring expansion, b) with inner ring expansion [10]; $K_i$, $K_o$ – contact stiffness of inner race (i) and outer race (o), $K_r$ – elastic stiffness of inner ring, $F_r$ – elastic force due to inner ring deformation, $\delta_i$, $\delta_o$ – contact deformation, $\delta_P$ – elastic deformation of inner ring, $x_k$ – ball displacement*

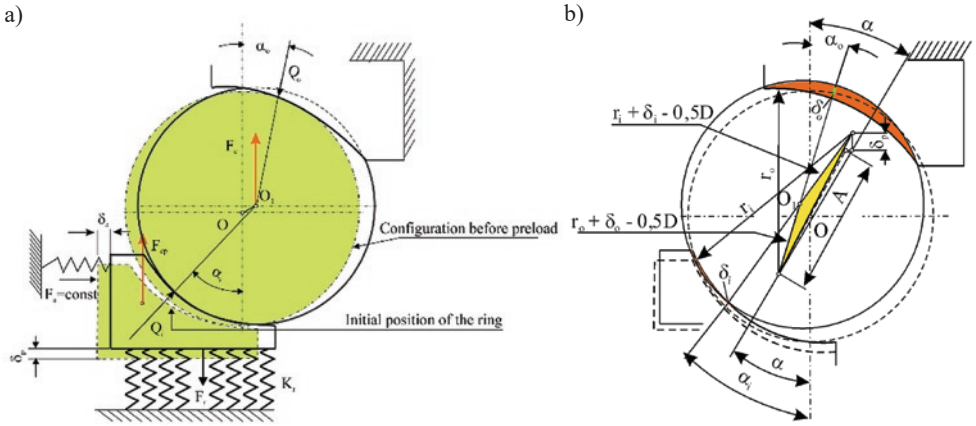


*Fig. 4. The state of a bearing load taking into account centrifugal load due to orbital movement of balls $F_c$ and due to rotation of inner ring $F_{cp}$*

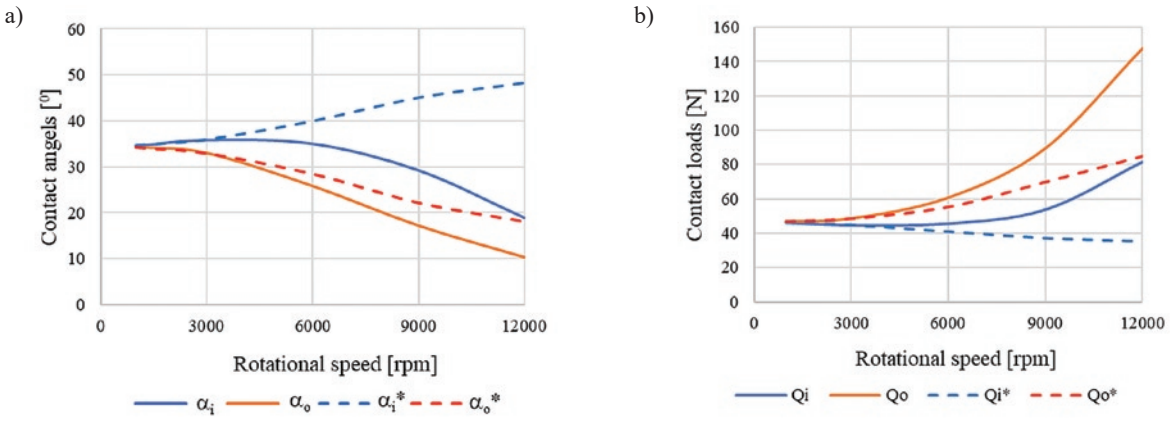


*Fig. 5. The influence of rotational speed on contact angels αi and αo and contact loads $Q_i$ and $Q_o$ [10]: continuous line relates to the model without expansion of the inner ring, dashed line relates to the model with expansion of the inner ring*

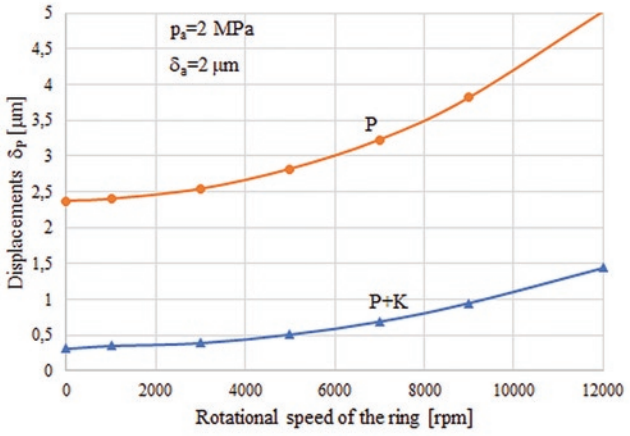


*Fig. 6. Displacements of the inner ring as a function of rotational speed: P – freely expansion of the inner ring, P+K – inner ring as a part of bearing*

$\delta_i$, $\delta_o$ – contact deformation of the ball in the area of the inner and outer race,
$\delta_P$ – radial displacement of the inner bearing ring,
$\alpha$, $\alpha_i$, $\alpha_o$ – contact angles,
$K_r$ – elasticity constant of the inner bearing ring,
$A$ –distance between the centers of the curvature of the inner and outer race (design feature of the bearing).

On this basis, it was possible to carry out simulation tests showing the influence, for example, of the rotational speed on contact forces $Q_i$ and $Q_o$ and on the contact angles $\alpha_i$ and $\alpha_o$ (Fig. 5).

Even a cursory analysis of Fig. 5 shows that both the contact angles and the contact forces for both the models (continuous lines in the charts refer to the extended model, i.e. the model in which the dynamic effects of the rotating inner ring are taken into account) - they vary by 20 - 30%.

The system of equations (3) and (4) also allows to compare the deformations of the inner ring as a function of the rotational speed for two, extremely different ring models, i.e. freely expanding under the influence of the centrifugal force and constituting a part of the bearing. Figure 6 shows strains $\delta_P$ of the ring at the point of its contact with the shaft, i.e. on the inner surface of the ring.

The deformations of the freely expanding ring (line P) are several times larger than the in the ring constituting the bearing element (line P + K). Therefore, corroborated is a critical opinion about improper ring modeling in [3], [7], [18, 19].

## 3. Effect of initial bearing pre-load and fit in the contact area of the shaft with the inner ring on contact forces

A vast majority of literature on contact phenomena in rolling bearings focuses on the effect of bearing speed and its elastic pre-load on the operating angles $\alpha_i$ and $\alpha_o$ and contact forces $Q_i$ and $Q_o$. On the other hand, there are almost no items that would consider the impact of the shaft and inner ring fit and pre-displacement of the bearing on the above parameters. Exceptions there to include items [11] and [17], where the authors analyzed the effect of rigid pre-displacement. To solve this problem analytically, they adopted a far-reaching simplification regarding the relationship between contact angles $\alpha_i$ and $\alpha_o$ (an assumption was made that $\alpha_i=\alpha+\Delta\alpha$ and $\alpha_o=\alpha-\Delta\alpha$). This simplification significantly distorts the calculation results of these angles and contact forces at high rotational speeds.

In engineering solutions for rolling bearings, especially angular bearings, two pre-load techniques are used (Figure 7). The first of them, referred to as a flexible, elastic pre-load, uses a spring or hydraulic element for pre-tensioning. This solution ensures a constant value of the pre-load of $F_a$ bearings. Modeling procedures performed according to this solution are simpler and allow an analytical determination of the parameters sought, and that is why it is more common in analytical research. In engineering practice, however, it is rarely used.

The other solution, most often found in engineering practice, referred to as initial stiff deformation, consists in axial displacement of the inner ring with respect to the outer one by a certain distance $\delta_a$ (several or a dozen or so μm).

The disadvantage of this solution is a changing axial force acting on the bearing, along with the changing speed. This structural solution is much more difficult to determine analytically such parameters as contact angles and contact forces, and that is why it is much less common in the literature. The author, in this article, presented some research results for such a solution.

The second important factor affecting contact forces $Q_i$, $Q_o$, and thus the resistance of the bearing movement is the fit between the shaft and the inner ring. In typical solutions of bearing assemblies of machine tool spindles, applied are fits causing negative clearance $\delta_P$. The size of this clearance ranges from a few to a dozen or so μm. There is no report in the literature about the impact of this fit on contact forces in the bearing. Therefore, the author conducted simulation studies, showing, among others, the effect of the negative clearance on the contact forces, especially in combination with the initial deformation (displacement) of the inner ring in relation to the outside ring $\delta_a$.

Because it is difficult to obtain an analytical solution without significant simplifications, as shown, among others in [11] and [17], in this work a numerical method – viz. the finite element method - has

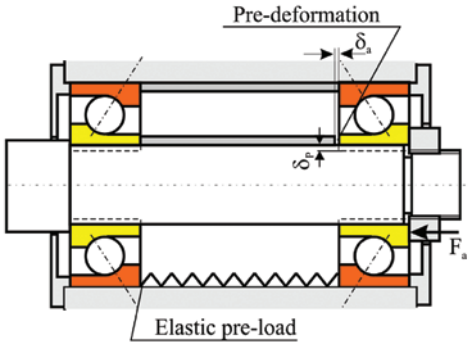


*Fig. 7. Methods of pre-load of an angular bearings; $\delta_a$ – pre-deformation, $F_a$ – elastic pre-load, $\delta_P$ – negative backlash due to close fit of shaft and bearing hole*

a)

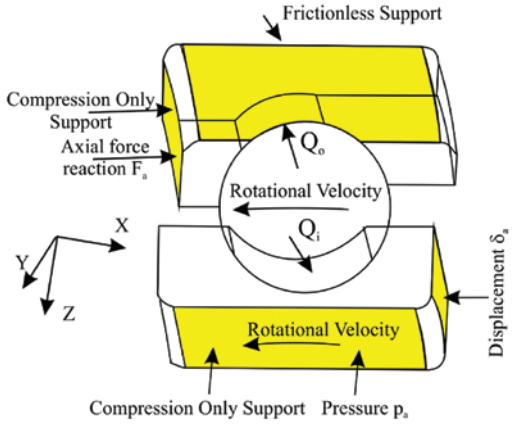


b)

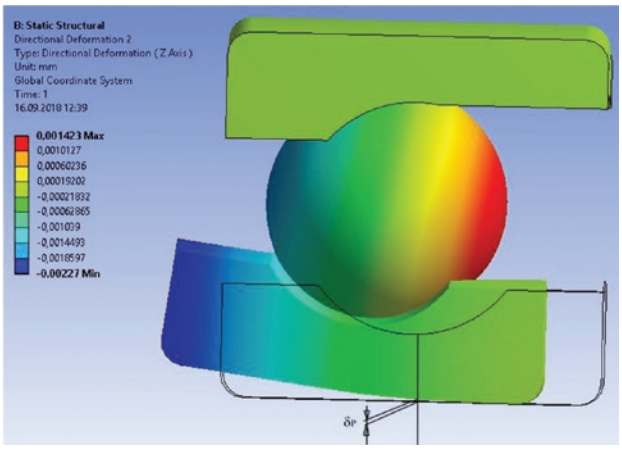


*Fig. 8. Geometrical model of a bearing for FEM simulation and an example of displacement distribution of a bearing model: $\delta_P$ – radial displacement of an inner ring*

been used, i.e. (Ansys 13). The geometrical model of the bearing is quite simple due to a large number of symmetry axes (Fig. 8). The boundary conditions were modeled as follows:

- *Compression Only Support* for the surface of the inner ring in contact with the shaft in the radial direction and for the surface of the outer ring in the axial direction,
- *Pressure* for the surface of the inner ring in contact with the shaft, to model the pressure *pa* from the negative clearance (fit) $\delta_P$,
- *Displacement* for the surface of the inner ring in the axial direction, in order to model the initial deformation $\delta_a$,
- *Frictionless Support* for the outer surface of the outer ring,
- *Contacts* for the contact area of balls with bearing races,
- *Rotational Velocity* in order to model the rotational motion of the inner ring and the orbital motion of the balls, and thus of centrifugal forces, too.

Figure 8 presents an example of the strain distribution and the method of determining a representative deformation $\delta_P$ for comparative purposes of test results. The model becomes deformed in each direction (X, Y, Z), but for the purpose of the analysis defined was a fixed measuring point (Fig. 8) in the Z direction (radial direction), corresponding to the radial deformation of the inner ring $\delta_P$.

From the point of view of the ongoing analysis, the following factors were of interest: the impact of the fit, expressed in the form of *Pressure pa* and initial deformation of *Displacement* $\delta_a$ on radial deformations $\delta_P$ (Figure 8) of the ring and consequently on contact forces $Q_i$ and $Q_o$. In addition, the influence of these parameters on the (*Axial force reaction*) $F_a$ (Fig. 8) on the ring's contact with the housing and the nut was also taken into account.

Figure 9a shows the relationship between pressure $p_a$ on the inner ring and the radial displacement $\delta_P$ of the ring for several systems. The dashed line refers to the standstill (n=0), i.e. a condition that will arise after assembly of the bearing with pre-determined $\delta_a$, and a continuous line at 12,000 rpm. The line applies to the freely expanding ring system (without a ball and an outer ring). Line P + K * applies to the bearing system only when the balls rotate in orbital motion. Instead, P + K line applies to the bearing system when the balls and the inner ring rotate. This figure allows one to estimate the relationship between the pressure which will occur on the inner ring and the negative clearance due to fit (displacement $\delta_P$ is associated with negative clearance due to fit).

This graph permits one to draw conclusions about the changing (increasing) radial displacement $\delta_P$ of the ring with increasing pressure Pa and speed (please compare the displacement for n = 12,000 revolutions per minute with the displacement after the assembly of the bearing n = 0 rev / min). It can also be stated that the failure to take into account the rotational motion of the ring (comparing P + K* and P + K) results in a significant pressure drop on the ring (for the selected fit). Fig. 9a shows an example for displacement $\delta_P$ = *2* µm. If you do not take into account the rotation of the ring (curve P + K*), then, pressure $p_a$ = *2* MPa. However, if we take into consideration the dynamic effects of the rotational movement of the ring (curve P + K), then, the pressure will be much higher, around 4.2 MPa.

Figure 9b shows the effect of $p_a$ pressure on the axial response of the $F_a$ in the contact areas of the bearing with the housing and the nut. It is possible to formulate a conclusion not only about a low impact of $p_a$ pressure on axial reactions $F_a$ or relatively large pre-displacements (for $\delta_a$=*20µm,* the fall in axial reaction does not exceed 10%) , but also on an intensified effect from pressure of *Pa* with decreasing pre-displacement (for $\delta_a$=*2µm,* the increase in

a)

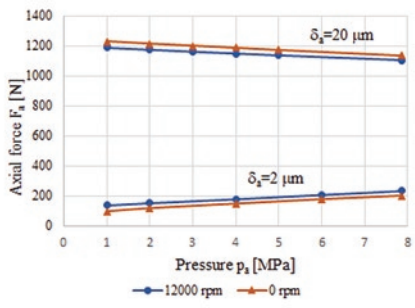


b)

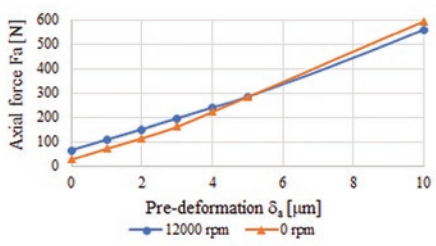


*Fig. 9. Influence of pressure $p_a$ on radial displacement $\delta_P$ of an inner ring and on axial force in the contact field of bearing and housing and a nut*

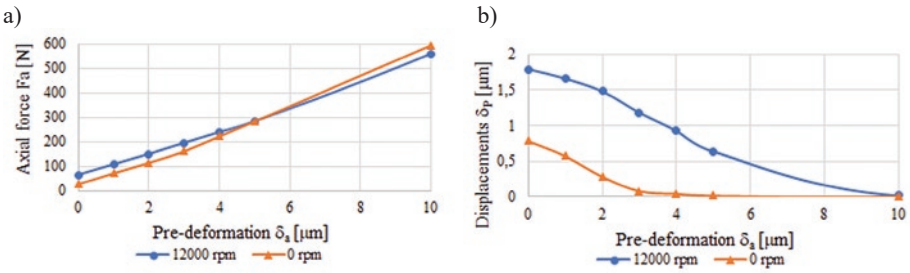


*Fig. 10. Effect of pre-deformation $\delta_a$ : a) on axial force $F_a$, b) on radial displacement of the ring $\delta_P$*

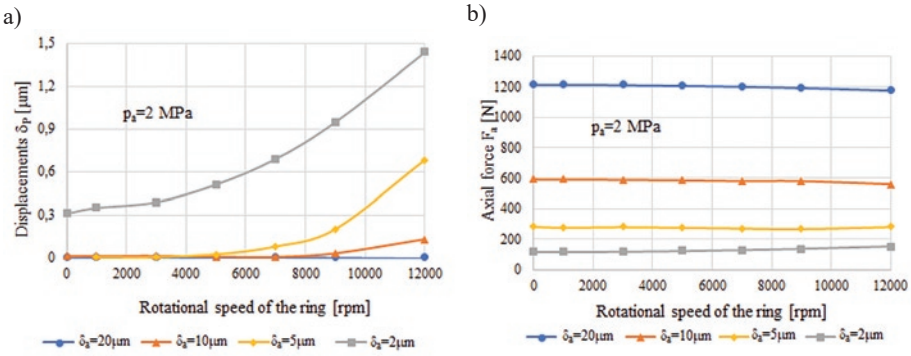


*Fig. 11. Effect of bearing speed a) on the radial displacement $\delta_P$ of the ring and b) on the axial force $F_a$*

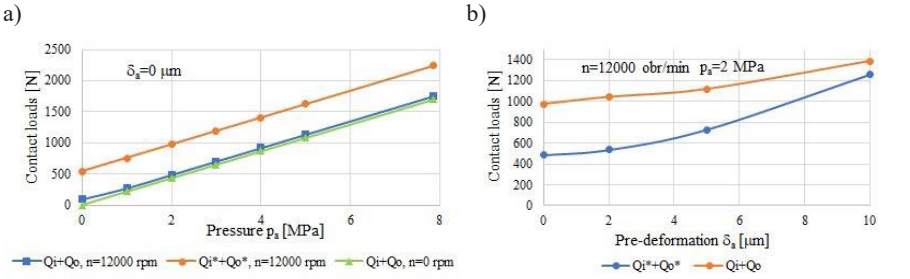


*Fig. 12. Effects from pressure $p_a$ and pre-deformation $\delta_a$ on contact loads, viz. on their sum: $Q_i + Q_o$ – with dynamic effects of the inner ring movement $Q_i^* + Q_o^*$ – without dynamic effects of the inner ring movement*

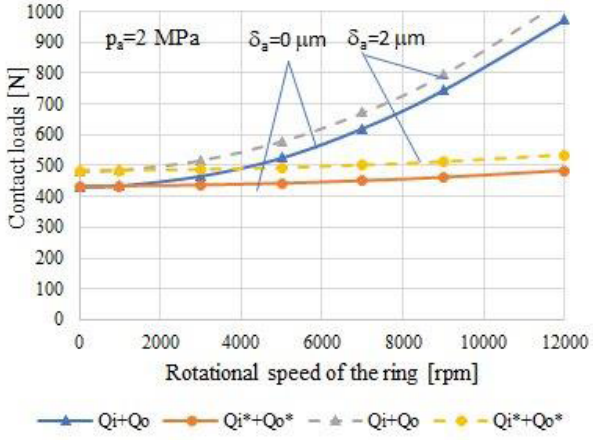


*Fig. 13. Effect from rotational speed on contact loads (their sum); $Q_i+Q_o$ – with dynamic effects of the inner ring movement, $Qi^*+Qo^*$ – without dynamic effects of the inner ring movement*

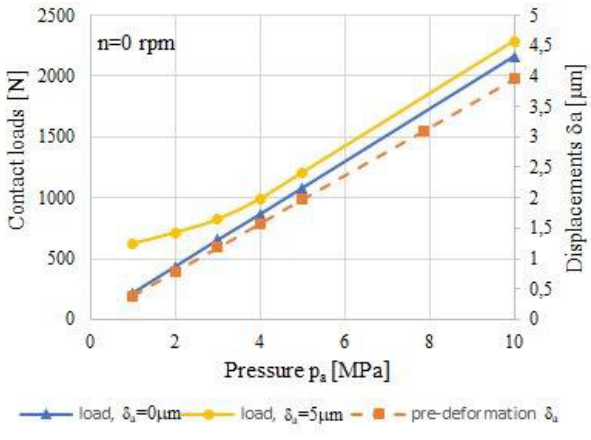


*Fig. 14. Effect from pressure $p_a$ on contact loads (their sum) and on radial displacement $\delta_P$ of the ring*

axial reaction reaches 80%). First of all, this reaction depends on the pre-displacement $\delta_a$.

The influence of pre-displacement $\delta_a$ on the radial displacements of the ring and on the axial reaction $F_a$ is shown in Fig. 10. Pre-deformations $\delta_a$ have a very strong influence on the axial response $F_a$. One might venture to call it a linear relationship. However, the influence of rotational speed seems to be insignificant.

The influence of pre-displacement $\delta_a$ on the radial displacement $\delta_P$ of the ring (Fig. 10b) depends significantly on the magnitude of this deformation and on the speed. Depending on the speed, as pre-displacement $\delta_a$, increases, the radial displacement of the ring decreases to a certain limiting value. Then, they do not change significantly as pre-displacement increases. For example, for a speed n = 0 rpm (condition after assembly of the bearing in the bearing seat), for deformations exceeding 3 μm, the displacement $\delta_P$ does not change any more . This is a valuable tip for a correct selection of assembly conditions for an angular bearing. It could be expected because the increase in the initial pre-load increases the axial stiffness of the bearing - and properly selected pre-displacement must guarantee mainly the required axial and radial stiffness. Often, the working temperature is also an important limitation.

Figure 10b shows that the bearing speed also affects the movement of the ring $\delta_P$ (compare displacements for *n=0* and *n=12000* rpm). Therefore, in the next illustration (Figure 11), in detail presented is the speed impact on the displacement $\delta_P$ (Figure 11a) and on the axial reaction $F_a$ (Figure 11b), too.

The conclusions from Figure 11a are interesting from the viewpoint of proper design of bearing assemblies. The effect of speed on radial displacements of the $\delta_P$ ring is generally strong. However, it depends essentially on the initial deformation of $\delta_a$. When the pre-displacement is increased during the assembly of a bearing, then, attenuated is the effect from the rotational speed on the radial displacements of the $\delta_P$ ring. For example, by increasing pre-displacement $\delta_a$ from 2 μm to 5 μm, radial displacements $\delta_P$ of the ring at a bearing speed of 12,000 rpm will decrease by approx. 75%. For a pre-displacement exceeding

10μm it can be assumed that the rotational speed does not significantly affect the radial deformations of the $\delta_P$ ring.

Instead, the rotational speed has no significant effect on the axial reaction of $F_a$ (Figure 11b). This reaction depends mainly on pre-displacement $\delta_a$.

The main purpose of the article is to assess the bearing movement resistance basing upon the calculated contact forces. Therefore, afterwards presented are the results of the research into the effects caused, respectively, by pressure $p_a$, pre-deformation $\delta_a$, and speed on contact forces (on their sum). Figure 12 shows the effect of pressure $Pa$ and pre-deformation $\delta a$ corresponding to a speed of 12,000 rpm

The impact of both parameters is significant. Contact forces (their sum) increase linearly with the pressure $p_a$, where the dynamic effect of the gyrating ring becomes evident when we compare the results for $Q_i + Q_o$ and $Q_i^* + Q_o^*$.

And so it is with pre-displacement $\delta_a$ (Fig. 12b). An increase in this parameter contributes to a significant increase in the sum of contact forces. The effect from the gyrating ring is as strong as it is when assessing the effect of pressure $p_a$.

Figure 13 shows the effect of rotational speed on contact forces, and in Figure 14 presented is an effect of pressure $p_a$ on contact forces and radial deformations $\delta_P$ of the ring, for a zero bearing speed. Thus, this is the condition of the bearing after its assembly in the bearing seat.

Simulation tests whose results are illustrated in Figure 13 prove that the differences between the contact forces (their sum) and thus the bearing movement resistance caused by rolling friction of balls on the raceways, while taking and not taking into account the dynamic effects of the gyrating ring and depending on the rotational speed, may reach 100% (for n = 12,000 rpm). It can be ascertained that when the dynamic influence of the rotating ring is neglected, this will significantly underestimate the contact forces, and thus the resistance to a bearing's motion. These results corroborate the thesis that pre-deformation $\delta_a$ affects contact forces. Figure 13 shows the test results for $\delta_a$=0 and 2μm, i.e. for a relatively small pre-strain; nevertheless, the differences can reach 10%.

In turn, Figure 14 shows the effect from $p_a$ pressure on contact forces (their sum) and on radial deformations $\delta_P$ of the ring for a speed n = 0 rpm, i.e. for the state after assembling the bearing in the bearing seat. This effect is unambiguously large.

Figure 14 also shows the relationship between pressure $p_a$ and pre-displacement $\delta_a$. This allows an estimation of one of these quantities, e.g. pressure $p_a$, for the pre-displacement $\delta_a$.

To sum it up, the designer of a bearing assembly, wanting to estimate the motion resistance, must take into account not only the dynamic effects caused by circulating balls, but also by the gyrating ring, pre-displacement $\delta_a$ of the bearing and fit of the shaft and bearing ring (in this case -pressure $p_a$). Failure to take these phenomena into account will result in errors in bearing resistance estimation of an order of 100% and more to the disadvantage, i.e. the estimated resistance will be lower than in reality.

## 4. Summary

The article presents the problem of angular bearing modeling in the context of its resistance to motion. It was assumed that the resistance caused by the friction of the balls on the raceways is a function of the contact forces occurring between the balls and raceways. Hence, the development of a model allowing the determination of these forces will play a pre-eminent role.

The article focuses on those factors which are so far have been poorly presented in the literature, i.e. the effect of dynamic phenomena related to the rotational movement of the bearing ring, with the effect of fit of the shaft in the bearing bore, with the effect of pre-displacement of the angular bearing upon contact forces and the radial deformation of the inner ring.

As a result of the MES numerical simulation research, the following has been ascertained:

– a significant effect of rotary motion of the inner ring on contact forces which, depending on the rotational speed of the bearing, can reach up to 100% if compared to the forces caused only by the orbital motion of the balls,

– a significant effect of pre-displacement $\delta_a$ of the bearing upon contact forces. For example, for a FAG 70B13-E test bearing, for every 1μm of pre-deformation, the contact force increase per one ball was about 40N (in the test bearing, there were 19 balls which resulted in an increase in contact forces of approx. 760 N). Since for test bearings typical values of pre-deformatioon can reach up to approx. 10μm, the resulting increase in contact forces is about 38% of the value corresponding to the contact forces due to centrifugal forces,

– a significant effect of fit in the form of a negative clearance on the value of contact forces.

## References


1. Alfares M A, Elsharkawy A. Effects of axial preloading of angular contact ball bearings on the dynamics of a grinding machine spindle system. Journal of Materials Processing Technology 2003; 136: 48-59, https://doi.org/10.1016/S0924-0136(02)00846-4.
2. Antoine F, Abba G, Molinari A. A new Proposal for Explicit Angle Calculation in Angular Contact Ball Bearing. Journal of Mechanical Design 2005;128 (2): 468-478, https://doi.org/10.1115/1.2168467.
3. Cao Hongrui, Chen Xuerfeng, He Zhengija: Study of characteristic variations of high-speed spindles induced by centrifugal expansion deformations. Journal of Vibroengineering 2012; 14(3): 1278-1292.
4. Chen J-S, Hwang Y-W. Centrifugal force induced dynamics of motorized high-speed spindle. Int. J. Ad. Manuf. Technol. 2006; 30: 10-19, https://doi.org/10.1007/s00170-005-0032-y.
5. Chudzik A, Warda B. Wpływ wewnętrznego luzu promieniowego na trwałość zmęczeniową promieniowego łożyska walcowego. Eksploatacja i Niezawodnosc - Maintenance and Reliability 2019; 2 (21): 1-20, https://doi.org/10.17531/ein.2019.2.4.
6. Harris T A, Kotzalas M N. Essential concepts of Bearing Technology. London: Taylor&Francis Group, 2007, https://doi.org/10.1201/9781420006599.
7. Itoigawa F, Nakamura T, Matsubara T. Starvation in ball bearing lubricated by oil and air lubrication system. Tribology for Energy Conservation/D. Dawson et al. (Editors), Elsevier Science B.V 1998; 243-252, https://doi.org/10.1016/S0167-8922(98)80079-5.
8. Jędrzejewski J, Kwaśny W. Modelling of angular contact ball bearings and axial displacements for high-speed spindles. CIRP Annals-Manufacturing Technology 2010; 59: 377-383, https://doi.org/10.1016/j.cirp.2010.03.026.
9. Kosmol J. Determination of motion resistances in high-speed spindle angular bearings. Monography. Gliwice: Silesian University of Technology, 2016.
10. Kosmol J. Extended contact model of angular bearing. Journal of Theoretical and Applied Mechanics 2019; 57(1): 59-72, https://doi.

org/10.15632/jtam-pl.57.1.59.
11. Liao N T, Lin J F. Ball bearing skidding under radial and axial loads. Mechanism and Machine Theory 2002; 37: 91-113, https://doi.org/10.1016/S0094-114X(01)00066-0.
12. Musiał J, Styp-Rekowski M. Analytical and experimental method of resistance motion coefficient determination in rolling friction. Proceedings of conference "Problems of unconventional bearing configuration", Łódź 1999: 59-65.
13. Noel D, Rithou M, Furet B, Leloch S. Complete Analytical Expression of the Stiffness Matrix of Angular Contact Ball Bearing. Journal of Tribology 2013; 135 (4): 04110-1- 04110-7, https://doi.org/10.1115/1.4024109.
14. Palmgren A. Łożyska toczne., Warszawa: PWT, 1951
15. Raczyński A, Kaczor J. Wpływ zacisku wstępnego łożysk kulkowych skośnych na trwałość łożyskowania. Zeszyty naukowe Politechniki Śląskiej Seria: Transport 2015; 83: 191-203.
16. Smolnicki T, Stańco M. Selected aspects of the maintenance of large-size rolling bearing. Eksploatacja i Niezawodnosc - Maintenance and Reliability 2009; 2 (42): 25-30.
17. Sum-Min Kim, Sun-Kuy Lee. Prediction of thermoelastic behavior in a spindle-bearing system considering bearing surroundings. International Journal of Machine Tools & Manufacture 2001; 41: 809-831, https://doi.org/10.1016/S0890-6955(00)00103-6.
18. Zivkovic A,. et al. A study of thermal behaviour of the machine tool spindle. Thermal Science 2018; 16, https://doi.org/10.2298/TSCI180129118Z.
19. Zivkovic A, Zivkovic M, Tabakovic S, Milojevic Z. Mathematical modelling and experimental testing of high-speed spindle behvior. Int J Adv Manuf Technol 2015; 77:1071-1086, https://doi.org/10.1007/s00170-014-6519-7.

**Jan KOSMOL**
Department of Machine Technology
Silesian University of Technology
ul. Konarskiego18A, 44-100 Gliwice, Poland

E-mail: jkosmol@polsl.pl